

Revisiting the flocking transition using active spins

A. P. Solon¹, J. Tailleur¹

¹ *Univ Paris Diderot, Sorbonne Paris Cite, MSC, UMR 7057 CNRS, F75205 Paris, France*

(Dated: October 29, 2018)

We consider an active Ising model in which spins both diffuse and align on lattice in one and two dimensions. The diffusion is biased so that plus or minus spins hop preferably to the left or to the right, which generates a flocking transition at low temperature/high density. We construct a coarse-grained description of the model that predicts this transition to be a first-order liquid-gas transition in the temperature-density ensemble, with a critical density sent to infinity. In this first-order phase transition, the magnetization is proportional to the liquid fraction and thus varies continuously throughout the phase diagram. Using microscopic simulations, we show that this theoretical prediction holds in 2d whereas the fluctuations alter the transition in 1d, preventing for instance any spontaneous symmetry breaking.

PACS numbers: 87.18.Gh, 05.65.+b, 45.70.Vn

Active matter systems are driven out-of-equilibrium by the injection of energy *at the single particle level* [1–4]. This microscopic breakdown of detailed-balance is responsible for a wide range of phenomena that have aroused the interest of physicists, from bacterial ratchets [5–8] to self-propelled clusters [9–11]. Furthermore, much of this rich phenomenology is captured by simple models. For instance, the patterns found in high density motility assays could be accounted for using simple flocking models [14, 15] while clustering in bacterial mixture was successfully modelled using self-propelled rods [16].

Nevertheless, despite the successful description of many experimental phenomena, a clear-cut understanding of the underlying mechanisms sometimes remain elusive. For instance, even though the flocking transition is one of the central features of active matter, it remains one of the most debated questions in the field. In their seminal work, Vicsek and co-workers [12] showed that self-propelled particles that align locally can exhibit a transition to long-range order in 2d. Initially thought to be continuous [12], this transition was later shown to be first order using large scale simulations and a finite-size-scaling akin to that of magnetic phase transitions [17]. Many works were also devoted to nematic [18–20] or metric-free interactions [21], the latter yielding a continuous transition [22]. Related flocking models were also studied in 1d [23, 24], where the transition was found to be continuous, casting even more confusion in the field. Beyond the presence of strong finite-size effects, a major difficulty in obtaining conclusive numerical evidence comes from the lack of a theoretical framework to analyse the finite-size scalings of flocking models.

In parallel to the numerical studies, much effort was thus devoted to the construction of such an analytical description of the flocking transition. While the Vicsek model (VM) is among the simplest to simulate, it is one of the hardest to coarse-grain, being defined off-lattice, in discrete time and involving many-body interactions. Many approaches were thus either phenomenological [13, 30, 32] or focused on simpler models [25], and progress is slower for the VM [26]. Lots of effort was again devoted to the

nematic case [27–29] or to topologic interactions [28, 31]. The existence of long-range order in 2d for polar alignment was established [13] but progress is difficult since the coarse-grained equations are hard to solve analytically. Most analytical studies were thus restricted to the linear stability analysis of homogeneous solutions or the simulation of coarse-grained equations [25, 30, 32]. While non-linear profiles for a model with *nematic alignment* could be computed analytically [28], closed analytical solutions are still missing for *polar models* despite recent progress [25, 26, 30]. All in all, in spite of the important progresses made during the last few years, a unifying theoretical framework of the flocking transition is still missing.

We present below a tentative step in this direction through the introduction of a microscopic lattice model with discrete symmetry, which is much simpler both to simulate and describe analytically than traditional flocking models. By bridging micro and macro, we show that the phase diagram of the flocking transition of our model amounts to a standard liquid-gas transition in the canonical ensemble *with a critical density* $\rho_c = \infty$. In particular, this sheds new light on the finite-size scaling of the transition and predicts the order parameter to vary *continuously* in the temperature-density plane, in the thermodynamic limit. Furthermore, we show that there is no continuous transition in 1d, where fluctuations strongly alter the transition.

Let us consider a one-dimensional lattice of L sites on which N particles have Ising spins $s = \pm 1$. Each particle hops asymmetrically at rate $D(1 + s\epsilon)$ and $D(1 - s\epsilon)$ to its right and left neighboring site. (In higher dimensions, the hopping rates are chosen symmetric in all directions but one.) There is no exclusion between particles and we note n_i^\pm the numbers of \pm spins on site i so that the local densities and magnetizations are given by $\rho_i = n_i^+ + n_i^-$ and $m_i = n_i^+ - n_i^-$. The particles also align their spins: on site i a spin s changes sign with rate $\exp(-s\beta \frac{m_i}{\rho_i})$ where $\beta \equiv 1/T$ plays the role of an inverse temperature [41]. When $D = 0$, the system thus amounts to L^d independent mean-field Ising models. When $D > 0$ and $\epsilon \neq 0$, three different configurations are typically found in the system

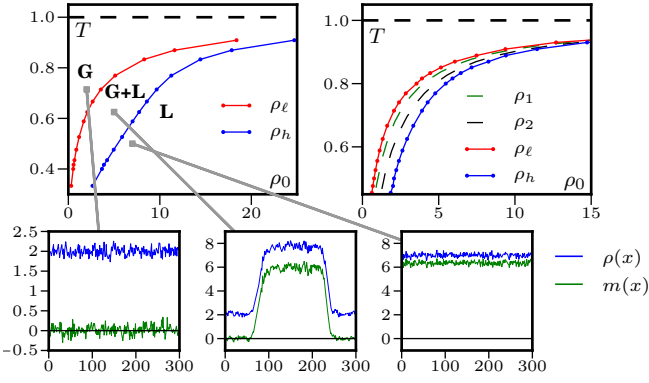


FIG. 1. **Top-left:** phase diagram in 2d with ordered liquid (L), disordered gas (G), and coexistence region (G+L). The red and blue lines correspond to low and high densities of phase separated profiles; they enclose the region where such profiles can be seen. $D = 1$, $\epsilon = 0.9$, $L = 300$, $\rho_0 = N/L$. **Bottom:** Snapshots of the different profiles averaged over the transverse direction. **Top-right:** Phase diagram predicted by the RMFM. In addition to ρ_h and ρ_ℓ , black and green dashed spinodal lines signal the loss of linear stability of the homogeneous profiles. $D = v = r = 1$.

(see Fig. 1): at low temperature a uniform ordered phase, at high temperature a uniform disordered phase, and in between a phase-separated system with high density ordered bands ($\rho_i \simeq \rho_h$, $m_i \simeq m_h \neq 0$) connected through narrow interfaces to a disordered homogeneous background ($\rho_i \simeq \rho_\ell$, $m_i \simeq 0$). The stability of these profiles in the thermodynamic limit depends on the number of spatial dimensions but they are all long-lived in finite systems. Let us now show how a simple theoretical framework can be constructed to account for the phase diagram of Fig. 1.

Many coarse-graining approaches used in the past rely on factorization approximation of microscopic kinetic equations [25, 27, 38, 39]. On a 1d lattice, this amounts to a simple mean-field approximation: $f(\langle n_i^\pm \rangle) = \langle f(n_i^\pm) \rangle$, which may be quantitatively wrong but often captures phase diagrams of lattice-gas models exactly [33] even in complicated cases [37]. Introducing continuous variables $x = i/L$, $v = 2D\epsilon/L$ and $\tilde{D} = D/L^2$, the mean-field dynamics of the coarse-grained fields $\rho(x) = \langle \rho_i \rangle$ and $m(x) = \langle m_i \rangle$ is given, in the large L limit, by

$$\dot{\rho} = \tilde{D}\partial_{xx}\rho - v\partial_x m \quad (1)$$

$$\dot{m} = \tilde{D}\partial_{xx}m - v\partial_x \rho + 2\rho \sinh \frac{\beta m}{\rho} - 2m \cosh \frac{\beta m}{\rho} \quad (2)$$

In higher dimensions, one simply replaces ∂_{xx} by a Laplacian Δ and we use this more general form hereafter.

Looking for the onset of a flocking transition, we linearize the dynamics for $m \ll \rho$, which yields [42]

$$\dot{m} = \tilde{D}\Delta m - v\partial_x \rho + 2m(\beta - 1) - \alpha \frac{m^3}{\rho^2} \quad (3)$$

where $\alpha = \beta^2(1 - \frac{\beta}{3})$. The profile $\rho(x) = \rho_0$, $m(x) = 0$ is thus linearly unstable for $\beta > 1$, where simulations of Eqs. (1)-(2) show that clusters are never stable [43] and always spread to reach the homogeneous ordered profile $m(x) = m_0$. Mean-field thus predicts a continuous transition from $m \equiv \frac{1}{L} \sum_i m_i = 0$ to $m = m_0(\beta)$ at $\beta_c = 1$, in clear contradictions with Fig. 1. As often [35, 36], this approximation is only valid for $\rho \rightarrow \infty$; for finite densities we thus expand the mean-field critical temperature to include $1/\rho$ corrections [44] and use $\beta_c \equiv 1 + \frac{r}{\rho}$ in Eq. 3:

$$\dot{m} = \tilde{D}\Delta m - v\partial_x \rho + 2m(\beta - 1 - \frac{r}{\rho}) - \alpha \frac{m^3}{\rho^2} \quad (4)$$

The phase diagram corresponding to Eqs. (1) and (4), which form our refined mean-field model (RMFM), is presented in the top-right corner of Fig. 1. When $T < 1$, homogeneous disordered (resp. ordered) profiles are always linearly stable at low enough density $\rho_0 < \rho_1$ (resp. high enough density $\rho_0 > \rho_2$). Since $\rho_1 < \rho_2$, there is a finite intermediate region $[\rho_1, \rho_2]$ where neither homogeneous profiles are stable. In this region, the system separates in two homogeneous phases connected with sharp fronts: a disordered region with low density $\rho_\ell < \rho_1$ and an ordered region with high density $\rho_h > \rho_2$ and $m_h \neq 0$.

Propagating shocks can be computed analytically when β is close to 1 by linearizing Eq. (4) around the density $\rho_1 = r/(\beta - 1)$ at which the homogeneous disordered profile becomes linearly unstable. We first solve Eq. (1), by neglecting the diffusion term in a reference frame moving at speed c , to get ρ as a function of m :

$$\rho(\mathbf{r}) = \rho_\ell + \frac{v}{c}m(\mathbf{r}) \quad (5)$$

Eqs. (4) and (5) then yields for m

$$\tilde{D}\Delta m + c(1 - \frac{v^2}{c^2})\partial_x m + \mu[\rho_\ell - \rho_1 + \frac{v}{c}m(x)]m - \alpha \frac{m^3}{\rho_1^2} = 0 \quad (6)$$

where $\mu = 2r/\rho_1^2$. Looking for ascending ($q^+ > 0$) and descending front ($q^- < 0$) solutions

$$m(\mathbf{r}) = \frac{m_h}{2}[1 + \tanh(q^\pm x)] \quad (7)$$

one gets

$$c = v \quad q^\pm = \pm \frac{m_h \sqrt{\alpha}}{\sqrt{8\tilde{D}\rho_1}} \quad m_h = \frac{4r}{3\alpha} \quad \rho_\ell = \rho_1 - \frac{4r}{9\alpha} \quad (8)$$

Such solutions are consistent with our approximations since $\frac{\rho - \rho_1}{\rho_1} \ll 1$ and $\tilde{D}\Delta \rho \ll v\partial_x \rho$ when $\beta \rightarrow 1$ [48]. In this regime, simulations of the RMFM and Eqs. (5-8) yield the same profiles and band velocities. For larger β , the $\tilde{D}\Delta \rho$ term makes front and rear interfaces asymmetric and $c > v$: the flocks fly faster than the birds [48].

Since ρ_ℓ , ρ_h and m_h do not depend on ρ_0 , increasing the average density at fixed temperature simply increases the fraction of the high-density region. In the thermodynamic

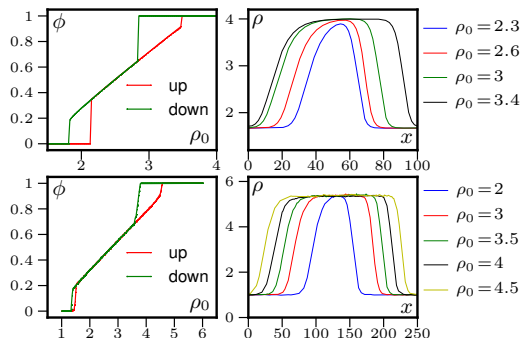


FIG. 2. **Left:** Fraction of the ordered liquid phase when ρ_0 is either increased or decreased for the RMFM (top) and in 2d microscopic simulations (bottom). **Right** Corresponding profiles of the system. **Parameters:** RMFM $L = 100$, $v = D = 1$, $r = 1.6$, $\beta = 1.75$, $\Delta\rho_0 = 10^{-2}$ every $\Delta t = 15000$; 2d lattice model $L = 250$, $\beta = 2$, $D = 1$, $\varepsilon = 0.9$, $\Delta\rho_0 = 10^{-2}$ every $\Delta t = 500$.

limit, phase separated profiles can be seen from ρ_ℓ to ρ_h . One always has $\rho_\ell < \rho_1 < \rho_2 < \rho_h$ so that the clusters and the homogeneous profiles are both linearly stable in the intervals $[\rho_\ell, \rho_1]$ and $[\rho_2, \rho_h]$.

The refined mean-field scenario thus resembles an equilibrium liquid-gas phase transition in the temperature-density ensemble, the total magnetization being proportional to the fraction of the liquid phase. Varying the density ρ_0 at fixed T , one indeed observes the traditional hysteresis loops shown in Fig. 2. Increasing ρ_0 , homogeneous disordered profiles are seen up to ρ_1 where a discontinuous jump takes the system into a phase-separated profile. A further density increase results in a widening of the liquid phase which almost fills the system when $\rho \lesssim \rho_h$. (The finite widths of the interfaces connecting ρ_ℓ and ρ_h prevent phase-separated profiles for ρ_0 close to $\rho_{\ell/h}$ in finite systems.) Going down, the homogeneous liquid phase remains metastable until $\rho_0 = \rho_2$ and discontinuously jumps to a coexistent state. The fraction of gas then increases until it fills the system at $\rho \simeq \rho_l$.

Unlike equilibrium liquid-gas transitions, dense and dilute phases in flocking models have different symmetries due to the coupling between density and orientation. One thus cannot circumvent the transition and continuously transform the system from a gas to a liquid: the transition line cannot stop at a finite point in the (T, ρ_0) plane and, indeed, the critical density is infinite. As far as we are aware, this has not been described for other flocking models [45] even though it should be generic and is consistent with published numerical results on the VM [17, 25].

Let us now turn to simulations of the 2d active Ising model. Beyond the structure of the phase diagram (see Fig. 1), the RMFM correctly captures the mechanism of the transition. The coexistence between homogeneous and phase-separated profiles is confirmed and changing ρ_0 at fixed β inside the coexistence region simply changes the fraction of the liquid phase (see Fig. 2 and [48]); the ve-

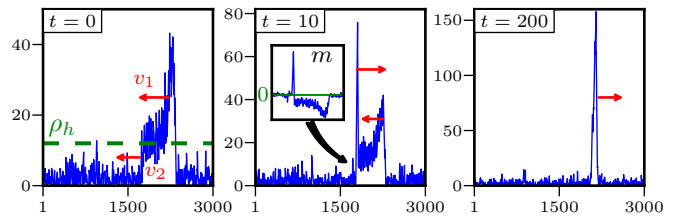


FIG. 3. Reversal of a 1d cluster due to a localized fluctuation. v_2 is greater than v_1 until $\rho(x) = \rho_h$ in the whole cluster. (See movies in [48].) $\rho_0 = 5$, $D = 1$, $\varepsilon = 0.9$, $\beta = 1.7$.

locity of the high density bands, for instance, remains constant [48]. Since the high density bands have a minimal size ℓ_c , the apparition of a flock in a finite-size system corresponds to a discontinuous jump to a non-zero magnetization $m_0 \simeq m_h \ell_c / L$ which vanishes as $L \rightarrow \infty$. As expected for a liquid-gas transition, the order parameter thus varies *continuously* throughout the phase diagram of the canonical ensemble, in the thermodynamic limit.

The scenario presented here can be related to the measurement of the binder cumulant $G = 1 - \frac{\langle m^4 \rangle}{3\langle m^2 \rangle^2}$ done in the literature [17, 29]. The coexistence between phase-separated profiles and supercooled gas phase yields a three-peak structure for $P(m)$ around $m = 0$ and $m = \pm m_0$ whose relative weights vary across the transition. (The same holds for the coexistence with superheated liquid.) Assuming a sum of three Gaussians of variance σ , the minimum of G , $G_{\min} = -[12(\sigma/m_0)^2 + 36(\sigma/m_0)^4]^{-1}$, is only markedly negative when $m_0 \gg \sigma$. Contrary to what happens in a grand-canonical ensemble, *both* m_0 and σ vanish when $L \rightarrow \infty$, the negative peak does not necessarily become more pronounced as $L \rightarrow \infty$, and one can easily mistake a first-order transition for a 2nd order one if σ remains comparable to m_0 (see the 1d case below).

Let us now show that fluctuations strongly alter the transition in 1d. First, all three profiles shown on Fig. 1 exist and are linearly stable in finite systems [46]. The general scenario predicted by the RMFM thus holds: homogeneous profiles between $\rho_1(T)$ and $\rho_2(T)$ are linearly unstable and tend to phase-separate between linearly stable low-density disordered regions and high-density ordered regions.

To assess the impact of fluctuations, let us consider the flipping of an ordered domain in the coexistence region. In 1d, an excess of, say, positive spins on *a single site* suffices to flip an approaching negative cluster (see Fig. 3); this happens frequently and the total magnetization keeps flipping in this region. The 2d counterpart of such a fluctuation is an excess of positive spins on *a transverse band of $\sim L$ sites* in front of the approaching cluster, which has a negligible probability when $L \rightarrow \infty$. Similarly, the $m = m_0$ homogeneous profile is unstable in the thermodynamic limit in 1d, which may be why it has not been observed before [46]. Indeed, even though a fluctuation that would create a small negative cluster in a uniform profile

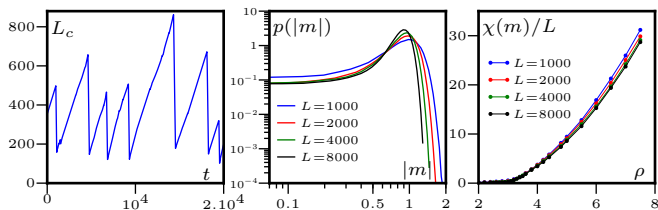


FIG. 4. **Left:** Cluster length as a function of time, showing a linear spreading between reversals. $D = 1$, $\varepsilon = 0.9$, $\beta = 2$, $\rho_0 = 3$. **Center & Right:** $P(|m|)$ for $\rho_0 = 4$; $\chi_m(\rho)/L$; $\beta = 1.538$, $D = 1$, $\varepsilon = 0.9$.

$m = m_0 > 0$ is rare, its probability does not decay exponentially fast with L since only a finite number of sites have to be flipped. When L increases, so does the entropy of such localized perturbations, and the time it takes to exit the homogeneous state thus vanishes when $L \rightarrow \infty$.

In 1d, there are thus only two phases in the thermodynamic limit: homogeneous disordered profiles and constantly flipping clusters of opposite magnetization, whose dynamics we now describe. Starting from a localized cluster, the ordered region spreads at constant speed (Fig. 4): the fore front is initially faster than the rear front and their velocity becomes equal only when the density in the band is uniformly equal to ρ_h (Fig. 3 and movies in [48]). The mean cluster size before a reversal, L_c^R , is thus proportional to the mean time between reversals, $\tau_R(L)$. The reversal then starts when a fluctuation at the front of the cluster begins to progressively flip all its sites (Fig. 3). It ends when this fluctuation has travelled through the whole cluster; this takes a time proportional to L_c^R and thus to $\tau_R(L)$. In the large size limit, the ratio of the probability of finding the system in a cluster or in a reversal is thus constant since both the times spent between and during reversals are $\propto \tau_R(L)$. $P(m)$ thus has a non-vanishing flat part between $\pm m_0$ and $\langle m \rangle = 0$ (Fig. 4): there is no spontaneous symmetry breaking in 1d. Consequently, the susceptibility $\chi_m = L(\langle m^2 \rangle - \langle m \rangle^2)$ is extensive in the cluster region, as can be seen in Fig. 4. Note that since the reversals capture a finite part of the steady-state measure, one should probably not use $|m|$ instead of m when computing χ_m , as is frequently done for the Ising model and was done in earlier studies of 1d flocking models.

The difficulty of analyzing Binder cumulants can be clearly seen in 1d, where the large L limit is easily reached and the three peaks in $P(m)$ at the transition can be very difficult to discriminate. If the width of the peaks σ is larger than their separation m_0 , no negative peak in G is observed and increasing L does not help since the peaks get closer as they get narrower. In figure 5 we show two extreme cases: without the RMFM to analyse the data, it would be very difficult to realize that one is looking at the same transition. This may explain why previous studies of 1d flocking models with similar—though not identical—dynamics concluded to a second-order transition [23, 24].

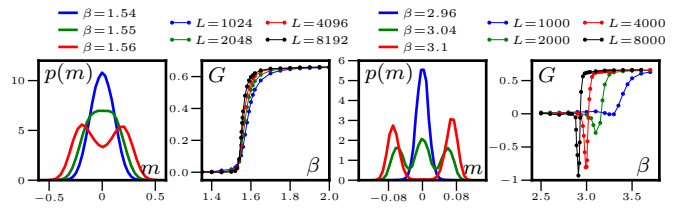


FIG. 5. Histograms and Binder cumulant of the total magnetization for $\rho_0 = 3$, $D = 1$ (left) and $\rho_0 = 0.2$, $D = 10$ (right). $\varepsilon = 0.9$. $L = 8000$ for $P(m)$.

Conclusion In this letter we have introduced a lattice model of self-propelled Ising spins, whose phenomenology is very similar to that of traditional models of aligning self-propelled particles. The simplicity of our model allows us to show that its flocking transition amounts to a liquid-gas phase transition in the canonical ensemble with an infinite critical density. The total magnetization is proportional to the liquid fraction and thus varies *continuously* through this first-order phase transition in the thermodynamic limit, a rather counter-intuitive result. This scenario, confirmed by numerical simulations in 2d, is altered by the strength of fluctuations in 1d, where neither spontaneous symmetry breaking nor continuous transitions are observed.

Despite fundamental differences between our model and others found in the literature, such as the symmetry of the order parameter, many features of the flocking transition observed here seem consistent with existing numerical results obtained either for microscopic models [17, 20, 28] or continuous descriptions [25, 26, 30, 32] of self-propelled particles. For instance, the phase diagram seems compatible with those of nematic [20, 28] or Vicsek models [17, 25], even though the high density regions have not been studied in these models. This suggests that the analogy between the flocking transition and a canonical liquid gas transition could be generic, while the symmetry of the order parameter would mostly control features of the ordered liquid phase. For instance, giant-number fluctuations, which have been reported in flocking models, are trivially present in the *coexistence region* of our model. There, $P(\rho_i)$ is double-peaked (around ρ_ℓ and ρ_h) and the variance of the number of particles in a box of finite size satisfies $\langle N^2 \rangle - \langle N \rangle^2 \propto \langle N \rangle^2$ [40]. They are however absent from the *homogeneous ordered phase* [48], which shows that such fluctuations are not intrinsic to polar flocking states.

The introduction of Active Spin models is clearly aimed at improving our theoretical understanding of the flocking transition rather than accounting for given experiments. One can nevertheless wonder whether such models could be relevant for experimental systems. Discrete symmetry of the order parameter can for instance stem out of a geometry which imposes only two possible flocking directions, as is the case for locusts constrained in a ring-shaped arena [49]. Then, as for the Vicsek model, the high density

region can only be attained if the interparticle interaction range is much larger than the particle size as can be the case, for instance, for electrostatic, hydrodynamic or social interactions. In other cases, such as hard rods, one cannot neglect the steric exclusion between particles and other density-induced effects which can strongly alter the flocking transition [38]. More generally, recent progresses on the manipulation of cold atoms in optical lattices have given a large freedom to control the interactions in spin chains [51]. This could provide an interesting path to build the quantum version of more general active spin models.

Last, part of the difficulty of analysing the transition comes from the “choice” of the temperature-density ensemble where no discontinuous jump of the magnetization is seen in the thermodynamic limit. The design of grand-canonical counterparts of flocking models, in which the magnetization would jump discontinuously at a transition line, thus seems a promising line of research, even though “changing ensemble” is not obvious out-of-equilibrium.

The authors thank M. Cheneau, H. Chaté, G. Grégoire, P. Krapivsky, F. Peruani, H. Touchette, F. van Wijland for useful discussions.

-
- [1] S. Ramaswamy, *Annu. Rev. Condens. Matter Phys.* **1**, 323 (2010)
- [2] P. Romanczuk, M. Br, W. Ebeling, B. Lindner, L. Schimansky-Geier, *Eur. Phys. J. Spec. Top.* **202**, 1(2012)
- [3] T. Vicsek, A. Zafeiris, *Phys. Rep.* **517**, 71 (2012)
- [4] M. E. Cates, *Rep. Prog. Phys.* **75** 042601 (2012)
- [5] P. Galajda, J. Keymer, P. Chaikin, R. Austin, J. Bacteriol. **189**, 8704 (2007); P. Galajda, J. Keymer, J. Dalland, S. Parkd, S. Koud, Rob. Austin, *J. Mod. Opt.* **55**, 3413 (2008)
- [6] J. Tailleur, M.E. Cates, *EPL* **86**, 60002 (2009)
- [7] L. Angelani, R. Di Leonardo, G. Ruocco, *Phys. Rev. Lett.* **102** 048104 (2009); R. Di Leonardo, L. Angelani, D. Dell’Arciprete, G. Ruocco, V. Iebba, S. Schippa, M. P. Conte, F. Mecarini, F. De Angelis, E. Di Fabrizio, *Proc. Natl. Acad. Sci. USA* **107** 9541 (2010)
- [8] A. Sokolov, M. M. Apodaca, B. A. Grzybowski, I. S. Aranson, *Proc. Natl. Acad. Sci. USA* **107** 969 (2010)
- [9] J. Schwarz-Linek, C. Valeriani, A. Cacciuto, M. E. Cates, D. Marenduzzo, A. N. Morozov, W. C. K. Poon, *Proc. Natl. Acad. Sci. USA* **109** 4052 (2012)
- [10] I. Theurkauff, C. Cottin-Bizonne, J. Palacci, C. Ybert, and L. Bocquet, *Phys. Rev. Lett.* **108** 268303 (2012)
- [11] J. Palacci, S. Sacanna, A. P. Steinberg, D. J. Pine, P. M. Chaikin, *Science* **339**, 936 (2013)
- [12] T. Vicsek, A. Czirók, E. Ben-Jacob, I. Cohen, O. Shochet, *Phys. Rev. Lett.* **75**, 1226 (1995)
- [13] J. Toner and Y. Tu, *Phys. Rev. Lett.* **75**, 4326 (1995); *Phys. Rev. E* **58**, 4828 (1998); J. Toner, *Phys. Rev. Lett.* **108**, 088102 (2012); *Phys. Rev. E* **86**, 031918 (2012)
- [14] V. Schaller, C. Weber, C. Semmrich, E. Frey, A. R. Bausch, *Proc. Natl. Acad. Sci. USA* **108** 19183 (2011);
- [15] Y. Sumino, K. H. Nagai, Y. Shitaka, D. Tanaka, K. Yoshikawa, H. Chaté, K. Oiwa *Nature* **483**, 448 (2012)
- [16] F. Peruani, J. Starruss, V. Jakovljevic, L. Sogaard-Andersen, A. Deutsch, M. Bär, *Phys. Rev. Lett.* **108**, 098102 (2012)
- [17] G. Grégoire, H. Chaté, *Phys. Rev. Lett.* **92** 025702 (2004); H. Chaté, F. Ginelli, G. Grégoire, F. Raynaud, *Phys. Rev. E* **77** 046113 (2008).
- [18] F. Peruani, A. Deutsch, M. Bär, *Phys. Rev. E* **74**, 030904 (2006)
- [19] A. Baskaran, M. C. Marchetti, *Phys. Rev. Lett.* **101**, 268101 (2008); *J. Stat. Mech.*, P04019 (2010)
- [20] F. Ginelli, F. Peruani, M. Bär, H. Chaté, *Phys. Rev. Lett.* **104**, 184502 (2010)
- [21] M. Ballerini, N. Cabibbo, R. Candelier, A. Cavagna, E. Cisbani, I. Giardina, V. Lecomte, A. Orlandi, G. Parisi, A. Procaccini, M. Viale, V. Zdravkovic, *Proc. Natl. Acad. Sci. USA* **105** 1232 (2008)
- [22] F. Ginelli, H. Chaté, *Phys. Rev. Lett.* **105**, 168103 (2010)
- [23] A. Czirók, A.-L. Barabási, T. Vicsek, *Phys. Rev. Lett.* **82**, 209 (1999)
- [24] O. J. O’Loan, M. R. Evans, *J. Phys. A* **32** L99 (1999)
- [25] E. Bertin, M. Droz, G. Grégoire, *Phys. Rev. E* **74** 022101 (2006); *J. Phys. A* **42** 445001 (2009)
- [26] T. Ihle, *Phys. Rev. E* **83**, 030901 (2011); arXiv:1304.0149
- [27] A. Baskaran, M. C. Marchetti, *Phys. Rev. E* **77**, 011920 (2008)
- [28] A. Peshkov, I. S. Aranson, E. Bertin, H. Chaté, F. Ginelli, *Phys. Rev. Lett.* **109**, 268701 (2012)
- [29] S. Ngo, F. Ginelli, H. Chaté, *Phys. Rev. E* **86**, 050101(R) (2012)
- [30] S. Mishra, A. Baskaran, M. C. Marchetti, *Phys. Rev. E* **81**, 061916 (2010)
- [31] Yen-Liang Chou, Rylan Wolfe, and Thomas Ihle *Phys. Rev. E* **86**, 021120
- [32] A. Gopinath, M. F. Hagan, M. C. Marchetti, A. Baskaran, *Phys. Rev. E* **85**, 061903 (2012)
- [33] R. A. Blythe, M. R. Evans, *J. Phys. A* **40**, R333 (2007)
- [34] W. Ketterle, N. J. Van Druten, *Phys. Rev. A* **54**, 656 (1996)
- [35] J. Tailleur, J. Kurchan, V. Lecomte, *J. Phys. A* **41**, 50500 (2008)
- [36] A. G. Thompson, J. Tailleur, M. E. Cates, R. A. Blythe, *J. Stat. Mech.* P02029 (2011)
- [37] M. R. Evans, Y. Kafri, K. E. P. Sugden, J. Tailleur, *J. Stat. Mech.* P06009 (2011)
- [38] F. D. C. Farrell, M. C. Marchetti, D. Marenduzzo, J. Tailleur, *Phys. Rev. Lett.* **108**, 248101 (2012)
- [39] I. S. Aranson, L. S. Tsimring, *Phys. Rev. E* **71**, 050901(R) (2005)
- [40] I. S. Aranson *et al.*, *Science* **320** 612 (2008)
- [41] The temperature in our model plays a role similar to that of the angular or vectorial noises in the usual Vicsek models [17].
- [42] For $\beta > 3$ we would need to expand (2) to higher orders.
- [43] All the simulations of continuous equations done in this paper rely on spectral methods and fully-implicit time-stepping.
- [44] See [48] for more details or [34] for a similar procedure in the context of Bose-Einstein condensation.
- [45] The phenomenological equations of [30, 32] focus on the role of propulsion speed and other nonlinearities and rely on a choice of parameters yielding finite spinodal density ($\rho_c = 1$ in [32]). Here, on the opposite, we account for the effect of temperature and we can thus describe the full phase

diagram in the ρ, T plane, whence predicting the $\rho_c = \infty$ critical point.

- [46] Homogeneous ordered phases were not reported in original studies of 1d flocking models—as far as we are aware—but we numerically checked that they are also present in the models of [23, 24].
- [47] See [24] for a discussion in another 1d flocking model.
- [48] See Supplemental Material at [URL will be inserted by publisher]
- [49] J. Buhl, D. J. T. Sumpter, I. D. Couzin, J. J. Hale, E. Despland, E. R. Miller, S. J. Simpson, *Science* **312**, 1402 (2006)
- [50] J. Deseigne, O. Dauchot, and H. Chat, *Phys. Rev. Lett.* **105**, 098001 (2010); C. A. Weber, and T. Hanke, J. Deseigne, S. Léonard, O. Dauchot, E. Frey, H. Chaté, *Phys. Rev. Lett.* **110**, 208001 (2013)
- [51] T. Fukuhara *et al.*, *Nat. Phys.* **9**, 235 (2013)
- [52] Biological systems would typically corresponds to the limit $\varepsilon = 1$.